3 Propagation of Optical Beams in Fibers[1]

3.0 INTRODUCTION

The silica glass fiber has become the most important transmission medium for long-distance, high-data-rate optical communication. It has caused what can be called with very little exaggeration a revolution in the art and practice of communication. This success is due mostly to the prediction [1] and realization [2] of low-loss fibers and to the ability to drastically reduce group velocity dispersion in such fibers so that extremely short optical pulses ($\sim 5 \times 10^{-12}$ s) undergo minimal spreading in propagation. Confined and lossless propagation in fibers is accomplished by total reflection from the dielectric interface between the core and the cladding. This requires that the index of refraction of the core be greater than that of the cladding. In this chapter we will investigate the mode characteristics of the circular dielectric waveguide. Both step-index waveguides and graded-index fibers will be analyzed. The exact hybrid modes of the step-index waveguide will be derived first, to be followed by a treatment of the linearly polarized mode, which is a very useful approximation. The Wentzel–Kramers–Brillouin (WKB) method is used to derive the approximate solution of the field and the propagation constants of the graded-index fibers. Modal dispersion, chromatic dispersion, and fiber attenuation are also dicussed.

[1] Major contributions to this chapter were made by P. Yeh.

3.1 WAVE EQUATIONS IN CYLINDRICAL COORDINATES

Since the refractive index profiles $n(r)$ of most fibers are cylindrically symmetric, it is convenient to use the cylindrical coordinate system. The field components are E_r, E_ϕ, E_z, H_ϕ, H_r, and H_z. The wave equation (2.4-3) assumes its simple form only for the Cartesian components of the field vectors. Since the unit vectors $\mathbf{a}_r$ and $\mathbf{a}_\phi$ are not constant vectors, the wave equations involving the transverse components are very complicated. The wave equation for the z component of the field vectors, however, remains simple,

$$(\nabla^2 + k^2)\begin{Bmatrix} E_z \\ H_z \end{Bmatrix} = 0 \tag{3.1-1}$$

where $k^2 = \omega^2 n^2/c^2$ and ∇^2 is the Laplacian operator given by

$$\nabla^2 = \frac{\partial^2}{\partial r^2} + \frac{1}{r}\frac{\partial}{\partial r} + \frac{1}{r^2}\frac{\partial^2}{\partial \phi^2} + \frac{\partial^2}{\partial z^2}$$

The problems of wave propagation in a cylindrical structure are usually approached by solving for E_z and H_z first and then expressing E_r, E_ϕ, H_r, and H_ϕ in terms of E_z and H_z.

Since we are concerned with the propagation along the waveguide, we assume

$$\begin{bmatrix} \mathbf{E}(\mathbf{r}, t) \\ \mathbf{H}(\mathbf{r}, t) \end{bmatrix} = \begin{bmatrix} \mathbf{E}(r, \phi) \\ \mathbf{H}(r, \phi) \end{bmatrix} \exp[i(\omega t - \beta z)] \tag{3.1-2}$$

i.e., every component of the field vector assumes the same z- and t-dependence of $\exp[i(\omega t - \beta z)]$. Maxwell's equations (3.1-1) and (3.1-2) are now written in terms of the cylindrical components and are given, respectively, by

$$i\omega\varepsilon E_r = i\beta H_\phi + \frac{1}{r}\frac{\partial}{\partial \phi} H_z \tag{3.1-3a}$$

$$i\omega\varepsilon E_\phi = -i\beta H_r - \frac{\partial}{\partial r} H_z \tag{3.1-3b}$$

$$i\omega\mu E_z = -\frac{1}{r}\frac{\partial}{\partial \phi} H_r + \frac{1}{r}\frac{\partial}{\partial r}(rH_\phi) \tag{3.1-3c}$$

and

$$-i\omega\mu H_r = i\beta E_\phi + \frac{1}{r}\frac{\partial}{\partial \phi} E_z \tag{3.1-4a}$$

$$-i\omega\mu H_\phi = -i\beta E_r - \frac{\partial}{\partial r} E_z \tag{3.1-4b}$$

$$-i\omega\mu H_z = -\frac{1}{r}\frac{\partial}{\partial \phi} E_r + \frac{1}{r}\frac{\partial}{\partial r}(rE_\phi) \tag{3.1-4c}$$

Using (3.1-3a), (3.1-3b), (3.1-4a), and (3.1-4b), we can solve for E_r, E_ϕ, H_r, and H_ϕ in terms of E_z and H_z. The results are

$$E_r = \frac{-i\beta}{\omega^2\mu\varepsilon - \beta^2}\left(\frac{\partial}{\partial r}E_z + \frac{\omega\mu}{\beta}\frac{\partial}{r\partial\phi}H_z\right)$$

$$E_\phi = \frac{-i\beta}{\omega^2\mu\varepsilon - \beta^2}\left(\frac{\partial}{r\partial\phi}E_z - \frac{\omega\mu}{\beta}\frac{\partial}{\partial r}H_z\right) \tag{3.1-5}$$

$$H_r = \frac{-i\beta}{\omega^2\mu\varepsilon - \beta^2}\left(\frac{\partial}{\partial r}H_z - \frac{\omega\varepsilon}{\beta}\frac{\partial}{r\partial\phi}E_z\right)$$

$$H_\phi = \frac{-i\beta}{\omega^2\mu\varepsilon - \beta^2}\left(\frac{\partial}{r\partial\phi}H_z + \frac{\omega\varepsilon}{\beta}\frac{\partial}{\partial r}E_z\right) \tag{3.1-6}$$

These relations show that it is sufficient to determine E_z and H_z in order to specify uniquely the wave solution. The remaining components can be calculated from (3.1-5) and (3.1-6).

With the assumed z-dependence of (3.1-2), the wave equation (3.1-1) becomes

$$\left[\frac{\partial^2}{\partial r^2} + \frac{1}{r}\frac{\partial}{\partial r} + \frac{1}{r^2}\frac{\partial^2}{\partial\phi^2} + (k^2 - \beta^2)\right]\begin{bmatrix}E_z\\H_z\end{bmatrix} = 0 \tag{3.1-7}$$

This equation is separable, and the solution takes the form

$$\begin{bmatrix}E_z\\H_z\end{bmatrix} = \psi(r)\exp(\pm il\phi) \tag{3.1-8}$$

where $l = 0, 1, 2, 3, \ldots$, so that E_z and H_z are single-valued functions of ϕ. Then (3.1-7) becomes

$$\frac{\partial^2\psi}{\partial r^2} + \frac{1}{r}\frac{\partial\psi}{\partial r} + \left(k^2 - \beta^2 - \frac{l^2}{r^2}\right)\psi = 0 \tag{3.1-9}$$

where $\psi = E_z, H_z$.

Equation (3.1-9) is the Bessel differential equation, and the solutions are called Bessel functions of order l. If $k^2 - \beta^2 > 0$, the general solution of (3.1-9) is

$$\psi(r) = c_1 J_l(hr) + c_2 Y_l(hr) \tag{3.1-10}$$

where $h^2 = k^2 - \beta^2$, c_1 and c_2 are constants, and J_l, Y_l are Bessel functions of the first and second kind, respectively, of order l. If $k^2 - \beta^2 < 0$, the general solution of (3.1-9) is

$$\psi(r) = c_1 I_l(qr) + c_2 K_l(qr) \tag{3.1-11}$$

where $q^2 = \beta^2 - k^2$, c_1 and c_2 are constants, and I_l, K_l are the modified Bessel functions of the first and second kind, respectively, of order l.

To proceed with our solution, we need the asymptotic forms of these functions for small and large arguments. Only leading terms will be given for simplicity.

For $x \ll 1$:

$$
\begin{aligned}
J_l(x) &\to \frac{1}{l!}\left(\frac{x}{2}\right)^l \\
Y_0(x) &\to \frac{2}{\pi}\left(\ln\frac{x}{2} + 0.5772\ldots\right) \\
Y_l(x) &\to -\frac{(l-1)!}{\pi}\left(\frac{2}{x}\right)^l \qquad l = 1, 2, 3, \ldots \\
I_l(x) &\to \frac{1}{l!}\left(\frac{x}{2}\right)^l \\
K_0(x) &\to -\left(\ln\frac{x}{2} + 0.5772\ldots\right) \\
K_l(x) &\to \frac{(l-1)!}{2}\left(\frac{2}{x}\right)^l \qquad l = 1, 2, 3, \ldots
\end{aligned}
\tag{3.1-12}
$$

For $x \gg 1, l$:

$$
\begin{aligned}
J_l(x) &\to \left(\frac{2}{\pi x}\right)^{1/2} \cos\left(x - \frac{l\pi}{2} - \frac{\pi}{4}\right) \\
Y_l(x) &\to \left(\frac{2}{\pi x}\right)^{1/2} \sin\left(x - \frac{l\pi}{2} - \frac{\pi}{4}\right) \\
I_l(x) &\to \left(\frac{1}{2\pi x}\right)^{1/2} e^{x} \\
K_l(x) &\to \left(\frac{\pi}{2x}\right)^{1/2} e^{-x}
\end{aligned}
\tag{3.1-13}
$$

In these formulas l is assumed to be a nonnegative integer. The transition from the small x behavior to the large x asymptotic form occurs in the region of $x \sim l$.

3.2 THE STEP-INDEX CIRCULAR WAVEGUIDE

The geometry of the step-index circular waveguide is shown in Figure 3-1. It consists of a core of refractive index n_1 and radius a, and a cladding of refractive index n_2 and radius b. The radius b of the cladding is usually chosen to be large enough so that the field of confined modes is virtually zero at $r = b$. In the calculation below we will put $b = \infty$; this is a legitimate assumption in most waveguides, as far as confined modes are concerned.

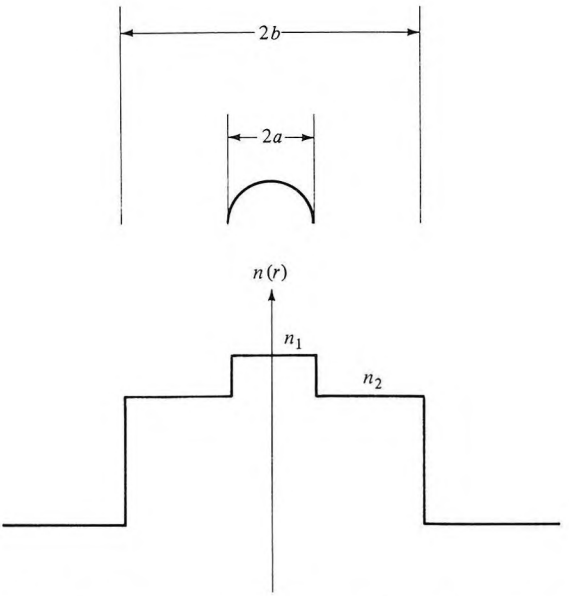

Figure 3-1 Structure and index profile of a step-index circular waveguide.

The radial dependence of the fields E_z and H_z is given by (3.1-10) or (3.1-11), depending on the sign of $k^2 - \beta^2$. For confined propagation, β must be larger than $n_2\omega/c$ (i.e., $\beta > n_2k_0 = n_2\omega/c$). This ensures that the wave is evanescent in the cladding region, $r > a$. The solution is thus given by (3.1-11) with $c_1 = 0$. This is evident from the asymptotic behavior for large r given by (3.1-13). The evanescent decay of the field also ensures that the power flow is along the direction of the z axis, i.e., no radial power flow exists. Thus the fields of a confined mode in the cladding ($r > a$) are given by

$$\begin{aligned} E_z(\mathbf{r}, t) &= CK_l(qr) \exp [i(\omega t + l\phi - \beta z)] \\ H_z(\mathbf{r}, t) &= DK_l(qr) \exp [i(\omega t + l\phi - \beta z)] \end{aligned} \qquad r > a \qquad \text{(3.2-1)}$$

where C and D are two arbitrary constants, and q is given by

$$q^2 = \beta^2 - n_2^2k_0^2$$

$$k_0 = \frac{\omega}{c} \qquad \text{(3.2-2)}$$

For the fields in the core, $r < a$, we must consider the behavior of the fields as $r \to 0$. According to (3.1-12), Y_l and K_l are divergent as $r \to 0$. Since the fields must remain finite at $r = 0$, the proper choice for the fields in the core ($r < a$) is (3.1-10) with $c_2 = 0$. This becomes evident only when matching, at the interface $r = a$, the tangential components of the field vectors **E** and **H** in the core with the cladding field components derived from (3.2-1); we

are unable to accomplish this if the radial dependence of the core fields is given by I_l. Thus the propagation constant β must be less than $n_1 k_0$, and the core fields are given by

$$\begin{aligned} E_z(\mathbf{r}, t) &= AJ_l(hr) \exp[i(\omega t + l\phi - \beta z)] \\ H_z(\mathbf{r}, t) &= BJ_l(hr) \exp[i(\omega t + l\phi - \beta z)] \end{aligned} \qquad r < a \qquad \text{(3.2-3)}$$

where A and B are two arbitrary constants, and h is given by

$$h^2 = n_1^2 k_0^2 - \beta^2 \qquad \text{(3.2-4)}$$

In the field expressions (3.2-1) and (3.2-3), we have taken a "+" sign in front of $l\phi$ in the exponents. A negative sign would yield a set of independent solutions, but with the same radial dependence. Physically, l plays a role similar to the quantum number describing the z component of the orbital angular momentum of an electron in a cylindrically symmetric potential field. Thus, if the positive sign in front of $l\phi$ corresponds to a clockwise "circulation" of photons about the z axis, the negative sign would correspond to a counterclockwise "circulation" of photons around the axis. Since the fiber itself does not possess any preferred sense of rotation, these two states are degenerate.

Equations (3.2-1) and (3.2-3) together require that $h^2 > 0$ and $q^2 > 0$, which translates to

$$n_1 k_0 > \beta > n_2 k_0 \qquad \text{(3.2-5)}$$

which can be regarded as a necessary condition for confined modes to exist. This is identical to the condition discussed in Section 13.1 for the slab dielectric waveguide and can be expected on intuitive grounds from our discussions of total internal reflection at a dielectric interface.

Using (3.2-1) and (3.2-3) in conjunction with (3.1-5) and (3.1-6), we can calculate all the field components in both the cladding and the core regions. The result is

Core ($r < a$):

$$\begin{aligned} E_r &= \frac{-i\beta}{h^2}\left[AhJ_l'(hr) + \frac{i\omega\mu l}{\beta r} BJ_l(hr)\right] \exp[i(\omega t + l\phi - \beta z)] \\ E_\phi &= \frac{-i\beta}{h^2}\left[\frac{il}{r} AJ_l(hr) - \frac{\omega\mu}{\beta} BhJ_l'(hr)\right] \exp[i(\omega t + l\phi - \beta z)] \\ E_z &= AJ_l(hr) \exp[i(\omega t + l\phi - \beta z)] \end{aligned} \qquad \text{(3.2-6)}$$

$$\begin{aligned} H_r &= \frac{-i\beta}{h^2}\left[BhJ_l'(hr) - \frac{i\omega\varepsilon_1 l}{\beta r} AJ_l(hr)\right] \exp[i(\omega t + l\phi - \beta z)] \\ H_\phi &= \frac{-i\beta}{h^2}\left[\frac{il}{r} BJ_l(hr) + \frac{\omega\varepsilon_1}{\beta} AhJ_l'(hr)\right] \exp[i(\omega t + l\phi - \beta z)] \\ H_z &= BJ_l(hr) \exp[i(\omega t + l\phi - \beta z)] \end{aligned} \qquad \text{(3.2-7)}$$

where

$$J_l'(hr) = dJ_l(hr)/d(hr),\ \varepsilon_1 = \varepsilon_0 n_1^2$$

Cladding ($r > a$):

$$E_r = \frac{i\beta}{q^2}\left[CqK_l'(qr) + \frac{i\omega\mu l}{\beta r}DK_l(qr)\right]\exp[i(\omega t + l\phi - \beta z)]$$

$$E_\phi = \frac{i\beta}{q^2}\left[\frac{il}{r}CK_l(qr) - \frac{\omega\mu}{\beta}DqK_l'(qr)\right]\exp[i(\omega t + l\phi - \beta z)]$$

$$E_z = CK_l(qr)\exp[i(\omega t + l\phi - \beta z)] \tag{3.2-8}$$

$$H_r = \frac{i\beta}{q^2}\left[DqK_l'(qr) - \frac{i\omega\varepsilon_2 l}{\beta r}CK_l(qr)\right]\exp[i(\omega t + l\phi - \beta z)]$$

$$H_\phi = \frac{i\beta}{q^2}\left[\frac{il}{r}DK_l(qr) + \frac{\omega\varepsilon_2}{\beta}CqK_l'(qr)\right]\exp[i(\omega t + l\phi - \beta z)]$$

$$H_z = DK_l(qr)\exp[i(\omega t + l\phi - \beta z)] \tag{3.2-9}$$

where $K_l'(qr) = dK_l(qr)/d(qr)$, $\varepsilon_2 = \varepsilon_0 n_2^2$. These fields must satisfy the boundary conditions that E_ϕ, E_z, H_ϕ, and H_z be continuous at $r = a$. This leads to

$$AJ_l(ha) - CK_l(qa) = 0$$

$$A\left[\frac{il}{h^2a}J_l(ha)\right] + B\left[-\frac{\omega\mu}{h\beta}J_l'(ha)\right] + C\left[\frac{il}{q^2a}K_l(qa)\right] + D\left[-\frac{\omega\mu}{q\beta}K_l'(qa)\right] = 0$$

$$BJ_l(ha) - DK_l(qa) = 0$$

$$A\left[\frac{\omega\epsilon_1}{h\beta}J_l'(ha)\right] + B\left[\frac{il}{h^2a}J_l(ha)\right] + C\left[\frac{\omega\varepsilon_2}{q\beta}K_l'(qa)\right] + D\left[\frac{il}{q^2a}K_l(qa)\right] = 0 \tag{3.2-10}$$

where the primes on J_l and K_l again refer to differentiation with respect to their arguments ha and qa, respectively. Equations (3.2-10) yield a nontrivial solution for A, B, C, and D, provided the determinant of their coefficients vanishes. This requirement yields the following mode condition that determines the propagation constant

$$\left(\frac{J_l'(ha)}{haJ_l(ha)} + \frac{K_l'(qa)}{qaK_l(qa)}\right)\left(\frac{n_1^2J_l'(ha)}{haJ_l(ha)} + \frac{n_2^2K_l'(qa)}{qaK_l(qa)}\right) = l^2\left[\left(\frac{1}{qa}\right)^2 + \left(\frac{1}{ha}\right)^2\right]^2\left(\frac{\beta}{k_0}\right)^2 \tag{3.2-11}$$

Equation (3.2-11), together with (3.2-4) and (3.2-2), is a transcendental function of β for each l. The function $J_l'(x)/xJ_l(x)$ in (3.2-11) is a rapidly varying

oscillatory function of $x = ha$. Therefore, (3.2-11) may be considered roughly as a quadratic equation in $J_l'(ha)/haJ_l(ha)$. For a given l and a given frequency ω, only a finite number of eigenvalues β can be found that satisfy (3.2-11) and (3.2-5). Once the eigenvalues have been found, we employ (3.2-10) to solve for the ratios B/A, C/A, and D/A that determine the six field components of the mode corresponding to each propagation constant β. These ratios are, from (3.2-10),

$$\begin{aligned}
\frac{C}{A} &= \frac{J_l(ha)}{K_l(qa)} \\
\frac{B}{A} &= \frac{i\beta l}{\omega\mu}\left(\frac{1}{q^2a^2} + \frac{1}{h^2a^2}\right)\left(\frac{J_l'(ha)}{haJ_l(ha)} + \frac{K_l'(qa)}{aqK_l(qa)}\right)^{-1} \\
\frac{D}{A} &= \frac{J_l(ha)}{K_l(qa)}\frac{B}{A}
\end{aligned} \tag{3.2-12}$$

The quantity B/A is of particular interest because it is a measure of the relative amount of E_z and H_z in a mode (i.e., $B/A = H_z/E_z$). Note that E_z and H_z are out of phase by $\pi/2$.

Mode Characteristics and Cutoff Conditions

In the treatment of slab waveguide modes in Section 13.2, we found that the solutions are easily separated into two classes, the TE and TM modes. In the circular waveguide, the solutions also separate into two classes. However, these are not in general TE or TM, each having in general nonvanishing E_z, H_z, E_ϕ, H_ϕ, E_r, and H_r components. The two classes in solutions can be obtained by noting that (3.2-11) is quadratic in $J_l'(ha)/haJ_l(ha)$, and when we solve for this quantity, we obtain two different equations corresponding to the two roots of the quadratic equation. The eigenvalues resulting from these two equations yield the two classes of solutions that are designated conventionally as the EH and HE modes.

By solving equation (3.2-11) for $J_l'(ha)/haJ_l(ha)$, we obtain

$$\begin{aligned}
\frac{J_l'(ha)}{haJ_l(ha)} = &-\left(\frac{n_1^2 + n_2^2}{2n_1^2}\right)\frac{K_l'}{qaK_l} \\
&\pm\left[\left(\frac{n_1^2 - n_2^2}{2n_1^2}\right)^2\left(\frac{K_l'}{qaK_l}\right)^2 + \frac{l^2}{n_1^2}\left(\frac{\beta}{k_0}\right)^2\left(\frac{1}{q^2a^2} + \frac{1}{h^2a^2}\right)^2\right]^{1/2}
\end{aligned} \tag{3.2-13}$$

where the arguments of K_l' and K_l are qa. We now use the Bessel function relations

$$\begin{aligned}
J_l'(x) &= -J_{l+1}(x) + \frac{l}{x}J_l(x) \\
J_l'(x) &= J_{l-1}(x) - \frac{l}{x}J_l(x)
\end{aligned} \tag{3.2-14}$$

and (3.2-13) becomes

EH modes:

$$\frac{J_{l+1}(ha)}{haJ_l(ha)} = \frac{n_1^2 + n_2^2}{2n_1^2}\frac{K_l'(qa)}{qaK_l(qa)} + \left(\frac{l}{(ha)^2} - R\right) \tag{3.2-15a}$$

HE modes:

$$\frac{J_{l-1}(ha)}{haJ_l(ha)} = -\left(\frac{n_1^2 + n_2^2}{2n_1^2}\right)\frac{K_l'(qa)}{qaK_l(qa)} + \left(\frac{l}{(ha)^2} - R\right) \tag{3.2-15b}$$

where

$$R = \left[\left(\frac{n_1^2 - n_2^2}{2n_1^2}\right)^2\left(\frac{K_l'(qa)}{qaK_l(qa)}\right)^2 + \left(\frac{l\beta}{n_1k_0}\right)^2\left(\frac{1}{q^2a^2} + \frac{1}{h^2a^2}\right)^2\right]^{1/2} \tag{3.2-16}$$

Equation (3.2-15) can be solved graphically by plotting both sides as functions of ha, letting $(qa)^2 = (n_1^2 - n_2^2)k_0^2a^2 - (ha)^2$ on the right-hand side.

We consider first the special case when $l = 0$. At $l = 0$ we have $\partial/\partial\phi = 0$, and all the field components of the modes are radially symmetric. There are two families of solutions that correspond to (3.2-15a) and (3.2-15b) above. In the first case, the mode condition (3.2-15a) becomes

$$\frac{J_1(ha)}{haJ_0(ha)} = -\frac{K_1(qa)}{qaK_0(qa)} \qquad \text{(TE)} \tag{3.2-17a}$$

where we used $K_0'(x) = -K_1(x)$. Under condition (3.2-17a), the constants A and C vanish according to (3.2-10) or (3.2-12). By substituting $A = C = 0$ and $l = 0$ in equations (3.2-6) through (3.2-9), we find that the only nonvanishing field components are H_r, H_z, and E_ϕ. These solutions are thus referred to as TE modes. If the eignevalues are β_m, $m = 1, 2, 3, \ldots$, the TE modes are designated as TE_{0m}, $m = 1, 2, 3, \ldots$, where the first subscript is $l = 0$.

In the second case, the mode condition (3.2-15b) at $l = 0$ becomes

$$\frac{J_1(ha)}{haJ_0(ha)} = -\frac{n_2^2K_1(qa)}{qan_1^2K_0(qa)} \qquad \text{(TM)} \tag{3.2-17b}$$

where we used $K_0'(x) = -K_1(x)$ and $J_{-1}(x) = -J_1(x)$. In this case the constants B and D vanish according to (3.2-10) or (3.2-12). By substituting $B = D = 0$ and $l = 0$ in equations (3.2-6) through (3.2-9), we find that the only nonvanishing field components are E_r, E_z, and H_ϕ. These solutions are thus referred to as TM modes and are designated as TM_{0m}.

Now consider the graphical solution of (3.2-17a) and (3.2-17b). Confined modes require that q be real to achieve the exponential decay of the field in the cladding. Thus we need only consider ha in the range $0 \le ha \le V \equiv k_0a(n_1^2 - n_2^2)^{1/2}$. The right-hand sides of (3.2-17) are always negative. Starting from $-K_1(V)/VK_0(V)$ for TE modes at $ha = 0$, the right side of (3.2-17a) is

a monotonically decreasing function of ha and becomes asymptotical, according to (3.1-12)

$$-\frac{K_1(qa)}{qaK_0(qa)} \xrightarrow[ha\to V]{} \frac{2}{(V^2 - h^2a^2)\ln(V^2 - h^2a^2)} \tag{3.2-18}$$

which diverges to $-\infty$ at $ha = V$. The right side of (3.2-17b) for TM modes behaves identically except for a factor of n_2^2/n_1^2. On the left sides of (3.2-17a) and (3.2-17b), $J_1(ha)/haJ_0(ha)$ starts from 1/2 at $ha = 0$ and increases monotonically until it diverges to ∞ at $ha = 2.405$, which is the first zero of $J_0(ha)$. Beyond $ha = 2.405$, $J_1(ha)/haJ_0(ha)$ varies from $-\infty$ to $+\infty$ between the zeros of $J_0(ha)$. For large values of ha, $J_1(ha)/haJ_0(ha)$ is a function resembling $-(ha)^{-1}\tan(ha - \pi/4)$, according to Figure 3-2 which shows the two curves describing the right and left sides of (3.2-17a), respectively. The normalized frequency $V = k_0a(n_1^2 - n_2^2)^{1/2}$ is assumed to be high enough so that two modes, marked by the circles at the intersection of the two curves, exist. The vertical asymptotes are given by the roots of $J_0(ha) = 0$. If the maximum value of ha, $(ha)_{max} = V$, is smaller than the first root of $J_0(x)$, 2.405, there can be no intersection of the two curves for real β. If V is between the first and the second zero of $J_0(x)$, there will be exactly one

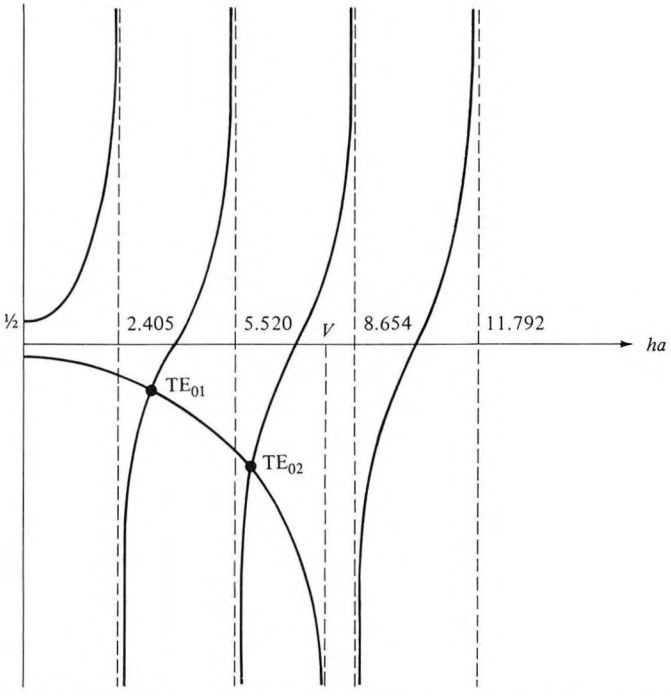

Figure 3-2 Graphical determination of the propagation constants of TE modes ($l = 0$) for a step-index waveguide.

intersection of the two curves. Thus the cutoff value (a/λ) for TE_{0m} (or TM_{0m}) waves is given by

$$\left(\frac{a}{\lambda}\right)_{0m} = \frac{x_{0m}}{2\pi(n_1^2 - n_2^2)^{1/2}} \tag{3.2-19}$$

where x_{0m} is the mth zero of $J_0(x)$. The first three zeros are

$$x_{01} = 2.405 \qquad x_{02} = 5.520 \qquad x_{03} = 8.654$$

For higher zeros, the asymptotic formula

$$x_{0m} \simeq (m - \tfrac{1}{4})\pi$$

gives adequate accuracy (to at least three figures).

When $l \neq 0$ in equations (3.2-15), the modes are no longer TE or TM but become the EH or HE modes of the waveguide. These can still be solved graphically in a manner similar to that outlined for the $l = 0$ case. For $l = 1$, the two curves representing the two sides of the EH mode condition (3.2-15a) are shown in Figure 3-3. The normalized frequency $V = k_0 a(n_1^2 - n_2^2)^{1/2}$ is assumed to be 8, so that there are two intersections. These are the EH_{11} and EH_{12} modes. The vertical asymptotes are given by the roots of $J_1(x) = 0$. Figure 3-4 shows those of the HE modes. At the same value of

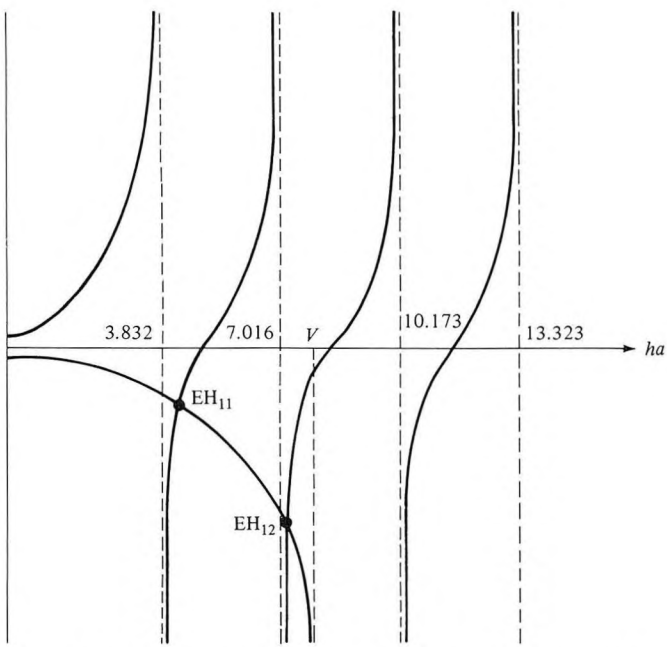

Figure 3-3 Graphical determination of the propagation constants of $l = 1$ EH modes for a step-index fiber.

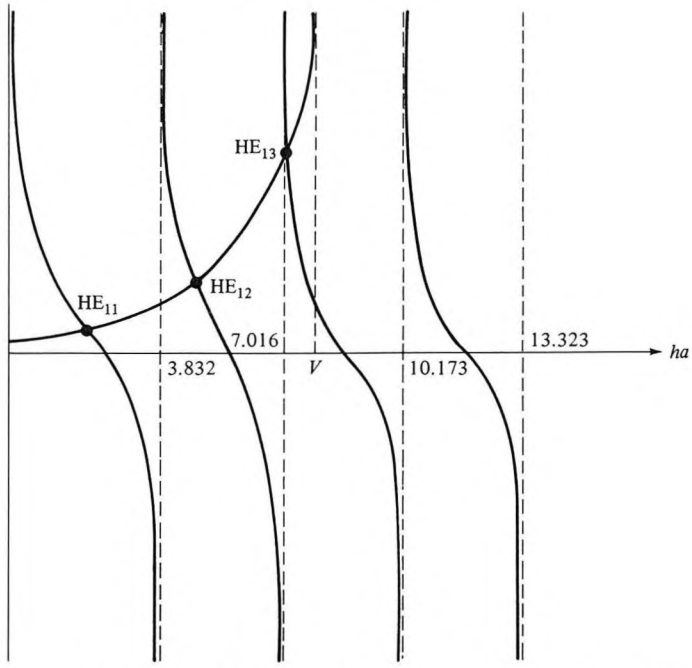

Figure 3-4 Graphical determination of the propagation constants of the $l = 1$ HE modes for a step-index dielectric waveguide.

$V = 8$ there are three intersections that correspond to HE_{11}, HE_{12}, and HE_{13} modes, respectively. The vertical asymptotes are also given by the roots of $J_1(x) = 0$. Note that, as shown in Figure 3-4, the intersection for HE_{11} mode always exists regardless of the value of V. This means the HE_{11} mode does not have a cutoff. All other HE_{1m}, EH_{1m} modes have cutoff values of a/λ given by

$$\left(\frac{a}{\lambda}\right)_{1m} = \frac{x_{1m'}}{2\pi(n_1^2 - n_2^2)^{1/2}} \tag{3.2-20}$$

where $m' = m$ for EH_{1m} modes and $m' = m - 1$ for HE_{1m} modes; x_{1m} is the mth zero of $J_1(x)$, excluding the one at $x = 0$. The first three zeros are

$$x_{11} = 3.832 \qquad x_{12} = 7.016 \qquad x_{13} = 10.173$$

For higher zeros, the asymptotic formula

$$x_{1m} \simeq m\pi + \frac{\pi}{4}$$

gives adequate accuracy (to at least three figures). For $l > 1$, the cutoff

values for a/λ are given by [3]

$$\left(\frac{a}{\lambda}\right)_{lm}^{\mathrm{EH}} = \frac{x_{lm}}{2\pi(n_1^2 - n_2^2)^{1/2}} \tag{3.2-21}$$

$$\left(\frac{a}{\lambda}\right)_{lm}^{\mathrm{HE}} = \frac{z_{lm}}{2\pi(n_1^2 - n_2^2)^{1/2}} \tag{3.2-22}$$

where x_{lm} is the mth zero of $J_l(x) = 0$, and z_{lm} is the mth root of

$$zJ_l(z) = (l - 1)\left(1 + \frac{n_1^2}{n_2^2}\right) J_{l-1}(z) \qquad l > 1 \tag{3.2-23}$$

If we substitute the propagation constant β for $l > 1$ into (3.2-12), we find that B/A is neither zero nor infinite. This means that both E_z and H_z are present in these modes. The designation of these hybrid modes is based on the relative contribution of E_z and H_z to a transverse component (e.g., E_r or E_ϕ) of the field at some reference point. If E_z makes the larger contribution, the mode is considered E-like and designated EH_{lm}, and so on. The mode HE_{11} can propagate at any wavelength, as noted earlier, since $(a/\lambda)_{11}^{\mathrm{HE}} = 0$. The next modes that can propagate, according to (3.2-19) are the TE_{01} and TM_{01} modes. Since x_{lm} or z_{lm} forms an increasing sequence for fixed l and increasing m, or for fixed m and increasing l, the number of allowed modes increases as the square of a/λ (see Problem 3.1).

For many applications, the important characteristic of a mode is the propagation constant β as a function of the frequency ω (or normalized frequency V). This information is often presented as the mode index of the confined mode

$$n = \frac{\beta}{k_0} \tag{3.2-24}$$

as a function of $V = k_0 a(n_1^2 - n_2^2)^{1/2}$; here $k_0 = \omega/c$. Since the phase velocity of a mode is ω/β, n is the ratio of the speed of light in vacuum to the mode phase velocity (n is also called the effective mode index). Figure 3-5 shows n for a number of the low-order modes of the step-index circular waveguide [4]. We note that at cutoff, each mode has a value of $(\beta/k_0) = n_2$. We can easily understand this by recalling that as the mode approaches cutoff, the fields extend well into the cladding layer. Thus, near cutoff the modes are poorly confined and most of the energy propagates in medium 2 and thus $n = n_2$. By similar reasoning, for frequencies far above cutoff, the mode is tightly confined to the core, and n approaches n_1.

As discussed earlier, for $V < 2.405$, only the fundamental HE_{11} mode can propagate. This is an important result, since for many applications single mode propagation is required. These applications include interferometry that calls for well-defined stationary phase fronts and optical communications by transmission of very short optical pulses. In the latter case the excitation of

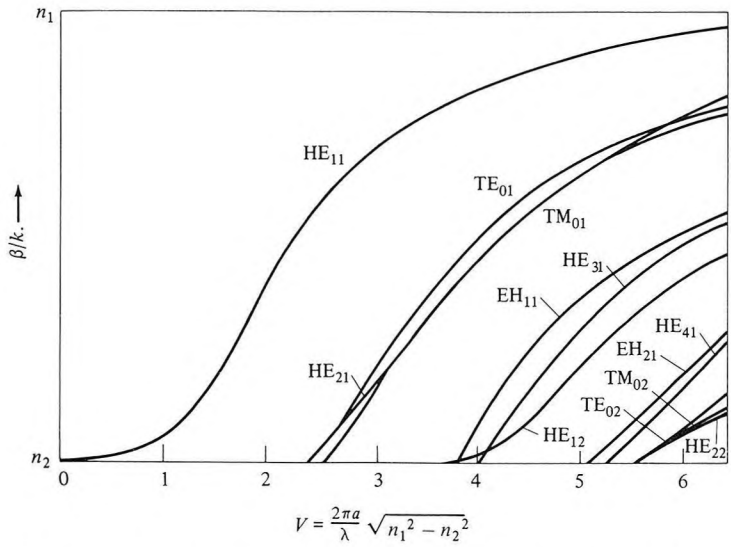

Figure 3-5 Normalized propagation constant as a function of V parameter for a few of the lowest-order modes of a step-index waveguide [4].

many modes would lead to pulse broadening, since the different modes possess different group velocities. This limits the number of pulses, i.e., bits, that can be packed into a given time slot and still be separable on the receiving end.

3.3 LINEARLY POLARIZED MODES

The mode condition (3.2-11) and the field components (3.2-6) through (3.2-9) and (3.2-12) are exact solutions of the wave equation (2.4-3) for the step-index dielectric waveguide. These exact expressions are very complicated especially for those hybrid modes (EH_{lm}, HE_{lm}) that have all six nonzero field components. A good approximation of the field components and mode condition can be obtained in most fibers whose core refractive index is only slightly higher than that of the cladding medium. Assuming that

$$n_1 - n_2 \ll 1 \tag{3.3-1}$$

the continuity condition on the tangential components of **H** at the interface between n_1 and n_2 becomes identical to that of the tangential components of the field vector **E**. This leads to a tremendous simplification in matching the field components at the core-cladding interface. Thus we may use the Cartesian components of the field vectors without introducing much complexity in solving the wave equation.

This simplified solution of the linearly polarized modes for the round fiber using the assumption (3.3-1) is due to Gloge [5]. In the limit (3.3-1), all the transverse wave numbers (h, q) are much smaller compared to the propagation constant β, i.e.,

$$q, h \ll \beta \tag{3.3-2}$$

We now start by solving the wave equation for the transverse Cartesian field components E_x, E_y, H_x, and H_y. These field components also satisfy the wave equations (3.1-7) and (3.1-9). For a step-index dielectric waveguide, the general solutions are given by (3.1-10) and (3.1-11). We now look for solutions where either the x or y component of the electric field vanishes. Since E_ϕ can be expressed in terms of E_x and E_y as

$$E_\phi = -E_x \sin \phi + E_y \cos \phi \tag{3.3-3}$$

it is apparent that E_ϕ component is simply proportional to either E_x or E_y. Thus the continuity of E_ϕ becomes equivalent to the continuity of E_x or E_y in these new solutions. Take the **E** field of a y-polarized solution of the form

$$E_x = 0 \tag{3.3-4}$$

$$E_y = \begin{cases} AJ_l(hr)e^{il\phi} \exp[i(\omega t - \beta z)] & r < a \\ BK_l(qr)e^{il\phi} \exp[i(\omega t - \beta z)] & r > a \end{cases} \tag{3.3-5}$$

where A and B are constants. We assume that $E_z \ll E_y$. The magnetic field components are then given, according to (2.4-1) and (3.1-2), by

$$\begin{aligned} H_x &= \frac{-i}{\omega\mu} \frac{\partial}{\partial z} E_y = \frac{-\beta}{\omega\mu} E_y \\ H_y &\simeq 0 \\ H_z &= \frac{i}{\omega\mu} \frac{\partial}{\partial x} E_y \end{aligned} \tag{3.3-6}$$

The longitudinal component of the electric field vector **E** is related to H_x, according to the Maxwell equation $\nabla \times \mathbf{H} = \varepsilon\, \partial\mathbf{E}/\partial t$

$$E_z = \frac{i}{\omega\varepsilon} \frac{\partial}{\partial y} H_x = \frac{-i\beta}{\omega^2\mu\varepsilon} \frac{\partial}{\partial y} E_y \tag{3.3-7}$$

where we used (3.3-6) in arriving at the last equality. We note that the field components E_x and H_y are zero in this solution. The other four field components can be expressed in terms of E_y. In order to calculate H_z and E_z, we need to carry out the differentiation with respect to x and y, respectively, according to (3.3-6) and (3.3-7). Since E_y is of the form (3.3-5), we need the relations

$$\frac{\partial}{\partial x} = \frac{\partial r}{\partial x} \frac{\partial}{\partial r} + \frac{\partial \phi}{\partial x} \frac{\partial}{\partial \phi} \tag{3.3-8}$$

and

$$\frac{\partial}{\partial y} = \frac{\partial r}{\partial y}\frac{\partial}{\partial r} + \frac{\partial \phi}{\partial y}\frac{\partial}{\partial \phi} \tag{3.3-9}$$

By using the definition of r and ϕ

$$r = (x^2 + y^2)^{1/2} \tag{3.3-10}$$

$$\phi = \tan^{-1}\left(\frac{y}{x}\right) \tag{3.3-11}$$

we obtain

$$\frac{\partial r}{\partial x} = \frac{x}{r} = \cos\phi \tag{3.3-12}$$

$$\frac{\partial r}{\partial y} = \frac{y}{r} = \sin\phi \tag{3.3-13}$$

$$\frac{\partial \phi}{\partial x} = -\frac{y}{r^2} = -\frac{1}{r}\sin\phi \tag{3.3-14}$$

and

$$\frac{\partial \phi}{\partial y} = \frac{x}{r^2} = \frac{1}{r}\cos\phi \tag{3.3-15}$$

We now substitute (3.3-5) for E_y in (3.3-6) and (3.3-7) and carry out the differentiation, using equations (3.3-8) through (3.3-15). After some laborious algebra and using the following functional relations of the Bessel function,

$$\begin{aligned} J_l'(x) &= \tfrac{1}{2}[J_{l-1}(x) - J_{l+1}(x)] \\ K_l'(x) &= -\tfrac{1}{2}[K_{l-1}(x) + K_{l+1}(x)] \end{aligned} \tag{3.3-16}$$

$$\begin{aligned} \frac{l}{x}J_l(x) &= \tfrac{1}{2}[J_{l-1}(x) + J_{l+1}(x)] \\ \frac{l}{x}K_l(x) &= -\tfrac{1}{2}[K_{l-1}(x) - K_{l+1}(x)] \end{aligned} \tag{3.3-17}$$

we obtain the following expressions for the field components.

Core ($r < a$):

$$\begin{aligned} E_x &= 0 \\ E_y &= AJ_l(hr)e^{il\phi}\exp[i(\omega t - \beta z)] \\ E_z &= \frac{h}{\beta}\frac{A}{2}[J_{l+1}(hr)e^{i(l+1)\phi} + J_{l-1}(hr)e^{i(l-1)\phi}]\exp[i(\omega t - \beta z)] \\ H_x &= -\frac{\beta}{\omega\mu}AJ_l(hr)e^{il\phi}\exp[i(\omega t - \beta z)] \\ H_y &\simeq 0 \\ H_z &= -\frac{ih}{\omega\mu}\frac{A}{2}[J_{l+1}(hr)e^{i(l+1)\phi} - J_{l-1}(hr)e^{i(l-1)\phi}]\exp[i(\omega t - \beta z)] \end{aligned} \tag{3.3-18}$$

Cladding ($r > a$):

$$E_x = 0$$

$$E_y = BK_l(qr)e^{il\phi} \exp[i(\omega t - \beta z)]$$

$$E_z = \frac{q}{\beta}\frac{B}{2}[K_{l+1}(qr)e^{i(l+1)\phi} - K_{l-1}(qr)e^{i(l-1)\phi}] \exp[i(\omega t - \beta z)]$$

$$H_x = -\frac{\beta}{\omega\mu} BK_l(qr)e^{il\phi} \exp[i(\omega t - \beta z)]$$

$$H_y \simeq 0$$

$$H_z = -\frac{iq}{\omega\mu}\frac{B}{2}[K_{l+1}(qr)e^{i(l+1)\phi} + K_{l-1}(qr)e^{i(l-1)\phi}] \exp[i(\omega t - \beta z)] \quad (3.3\text{-}19)$$

In arriving at (3.3-18) and (3.3-19), we have also used $\beta = n_1 k_0 \simeq n_2 k_0$, since $n_2 k_0 < \beta < n_1 k_0$ and $n_2 \to n_1$. Note that E_y and H_x are the dominant field components because in the limit (3.3-1) $h, q \ll \beta$. In other words, the field is essentially transverse. The constant B is given by

$$B = \frac{AJ_l(ha)}{K_l(qa)} \quad (3.3\text{-}20)$$

to ensure the continuity of $E_y(E_\phi \propto E_y)$ at the core boundary $r = a$. The constant A is then determined by the normalization condition.

The field solution (3.3-18) and (3.3-19) is a y-polarized wave ($E_x = 0$). For a complete field description, we also need the mode with the orthogonal polarization (i.e., an x-polarized wave). The field components E_x and E_y of this orthogonal mode are taken of the form

$$E_x = \begin{cases} AJ_l(hr)e^{il\phi} \exp[i(\omega t - \beta z)] & r < a \\ BK_l(qr)e^{il\phi} \exp[i(\omega t - \beta z)] & r > a \end{cases} \quad (3.3\text{-}21)$$

$$E_y = 0 \quad (3.3\text{-}22)$$

and the other field components are, according to the Maxwell equations,

$$E_z = \frac{-i}{\omega\varepsilon}\frac{\partial}{\partial x} H_y = \frac{-i\beta}{\omega^2\mu\varepsilon}\frac{\partial}{\partial x} E_x$$

$$H_x \simeq 0$$

$$H_y = \frac{i}{\omega\mu}\frac{\partial}{\partial z} E_x = \frac{\beta}{\omega\mu} E_x$$

$$H_z = \frac{-i}{\omega\mu}\frac{\partial}{\partial y} E_x \quad (3.3\text{-}23)$$

where we have assumed that $E_z \ll E_x$. We note that $E_y = 0$ and $H_x \simeq 0$ in this solution. By substituting (3.3-21) for E_x in (3.3-23) and carrying out the differentiation, using equations (3.3-8) through (3.3-15), we obtain, again

after some laborious algebra and using the relations (3.3-16) and (3.3-17), the following expressions for the field amplitudes:

Core ($r < a$):

$$
\begin{aligned}
E_x &= AJ_l(hr)e^{il\phi} \exp[i(\omega t - \beta z)] \\
E_y &= 0 \\
E_z &= i\frac{h}{\beta}\frac{A}{2}[J_{l+1}(hr)e^{i(l+1)\phi} - J_{l-1}(hr)e^{i(l-1)\phi}]\exp[i(\omega t - \beta z)] \\
H_x &\simeq 0 \\
H_y &= \frac{\beta}{\omega\mu} AJ_l(hr)e^{il\phi} \exp[i(\omega t - \beta z)] \\
H_z &= \frac{h}{\omega\mu}\frac{A}{2}[J_{l+1}(hr)e^{i(l+1)\phi} + J_{l-1}(hr)e^{i(l-1)\phi}]\exp[i(\omega t - \beta z)]
\end{aligned}
\tag{3.3-24}
$$

Cladding ($r > a$):

$$
\begin{aligned}
E_x &= BK_l(qr)e^{il\phi} \exp[i(\omega t - \beta z)] \\
E_y &= 0 \\
E_z &= i\frac{q}{\beta}\frac{B}{2}[K_{l+1}(qr)e^{i(l+1)\phi} + K_{l-1}(qr)e^{i(l-1)\phi}]\exp[i(\omega t - \beta z)] \\
H_x &\simeq 0 \\
H_y &= \frac{\beta}{\omega\mu} BK_l(qr)e^{il\phi} \exp[i(\omega t - \beta z)] \\
H_z &= \frac{q}{\omega\mu}\frac{B}{2}[K_{l+1}(qr)e^{i(l+1)\phi} - K_{l-1}(qr)e^{i(l-1)\phi}]\exp[i(\omega t - \beta z)]
\end{aligned}
\tag{3.3-25}
$$

In arriving at (3.3-24) and 3.3-25), we again made the assumption that $\beta \simeq n_1 k_0 \simeq n_2 k_0$ because of (3.3-1). We note that E_x and H_y are the dominant field components in this solution. Therefore, the mode is again nearly transverse and linearly polarized along the x direction. The constant B is again given by (3.3-20) to ensure the continuity of $E_x(E_\phi \propto E_x)$ at the core boundary $r = a$.

We have obtained the field expressions for two types of guided modes whose transverse fields are polarized orthogonally to each other. These field expressions are approximate solutions of Maxwell's equations, provided the tangential components of the field vectors are continuous at the dielectric interface $r = a$. The continuity of E_ϕ at $r = a$ leads to $B = AJ_l(ha)/K_l(qa)$ (3.3-20). The H_ϕ components are proportional to the E_ϕ components, according to the field expressions (3.3-18), (3.3-19), (3.3-24), and (3.3-25) in this approximation. Therefore the continuity of E_ϕ results in the continuity of H_ϕ.

We now consider the continuity of E_z at $r = a$. Since the continuity condition must hold for all azimuth angles ϕ, we must equate the coefficients of $\exp[i(l + 1)\phi]$ and $\exp[i(l - 1)\phi]$ separately. Using the field expressions (3.3-18) and (3.3-19) and (3.3-20), we obtain the following mode conditions:

$$h \frac{J_{l+1}(ha)}{J_l(ha)} = q \frac{K_{l+1}(qa)}{K_l(qa)} \tag{3.3-26}$$

and

$$h \frac{J_{l-1}(ha)}{J_l(ha)} = -q \frac{K_{l-1}(qa)}{K_l(qa)} \tag{3.3-27}$$

The same equations result from the continuity of H_z. In addition, if we use the field expressions (3.3-24) and (3.3-25) for the x-polarized mode, we will arrive at the same mode conditions (3.3-26) and (3.3-27). This means that these two transversely orthogonal modes are degenerate in the propagation constant β. The mode condition (3.3-27) is mathematically equivalent to (3.3-26) if we use the recurrence relation of the Bessel functions (3.3-17).

The mode condition (3.3-26) obtained in this approximation is much simpler than the exact expression (3.2-11). The exact mode condition (3.2-11) has twice as many solutions as the simple one (3.3-26) because (3.2-11) is quadratic in J_l'/J_l. This indicates that each solution of (3.3-26) is really twofold degenerate. In fact the propagation constants of the exact $HE_{l+1,m}$ and $EH_{l-1,m}$ modes are nearly degenerate [6]. They become exactly the same in the limit $n_1 \to n_2$. This can also be seen from the expressions of the field components E_z and H_z in (3.3-18), (3.3-19), (3.3-24), and (3.3-25). Comparison of the linearly polarized mode expressions with the exact modes (3.2-3) shows that the linearly polarized modes are actually a superposition of $HE_{l+1,m}$ and $EH_{l-1,m}$ modes [6]. Two independent linear superpositions lead to the x-polarized and y-polarized modes. The total number of modes is the same in both theories. The eigenvalues obtained from (3.3-26) are labeled as β_{lm} with $l = 0, 1, 2, 3, \ldots, m = 1, 2, 3, \ldots$, where the subscript m indicates the mth root of the transcendental equation (3.3-26). The modes are designated LP_{lm}. The lowest-order mode HE_{11} now has the propagation constant labeled β_{01} and the mode designated LP_{01}.

The mode conditions for those linearly polarized waves (3.3-26) or (3.3-27) can also be solved graphically. Figure 3-6 shows the normalized propagation constant as a function of the normalized frequency V. The mode cutoff corresponds to the condition $q = 0$ which, according to (3.3-27), leads to the condition

$$J_{l-1}(V) = 0 \tag{3.3-28}$$

where

$$V = k_0 a(n_1^2 - n_2^2)^{1/2} = 2\pi \frac{a}{\lambda} (n_1^2 - n_2^2)^{1/2} \tag{3.3-29}$$

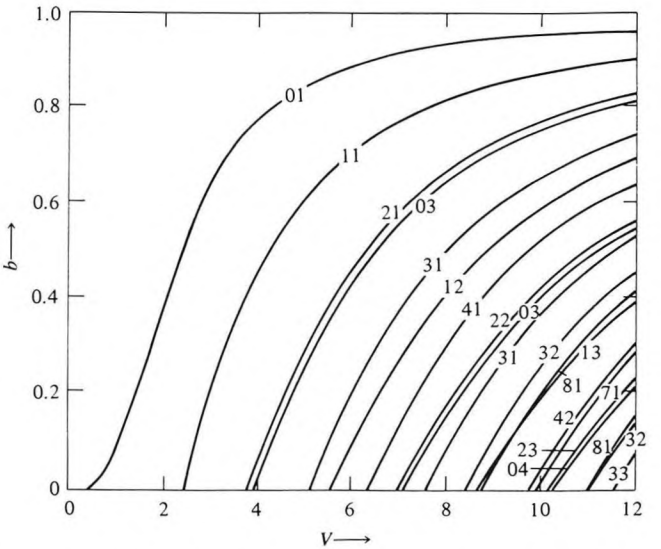

Figure 3-6 Normalized propagation constant b as function of normalized frequency V for the guided modes of the optical fiber, $b = (\beta/k_c - n_2)/(n_1 - n_2)$. (After Reference [5].)

It follows that the lowest-order mode, characterized by $l = 0$, has a cutoff given by the lowest root of the equation

$$J_{-1}(V) = -J_1(V) = 0 \qquad \text{(3.3-30)}$$

Hence $V = 0$. In other words, the lowest-order mode does not have a cutoff. This is the HE_{11} mode and is now labeled LP_{01}. The next mode of the type $l = 0$, cuts off when $J_1(V)$ next equals zero, that is, when $V = 3.832$. This mode is labeled LP_{02}. The cutoff values of V for some low-order LP_{lm} modes are given in Table 3-1. All these values are zeros of the Bessel function. For

Table 3-1 Cutoff Values of V for Some Low-Order LP Modes

V	$m = 1$	$m = 2$	$m = 3$	$m = 4$
$l = 0$	0	3.832	7.016	10.173
$l = 1$	2.405	5.520	8.654	11.792
$l = 2$	3.832	7.016	10.173	13.323
$l = 3$	5.136	8.417	11.620	14.796
$l = 4$	6.379	9.760	13.017	16.224

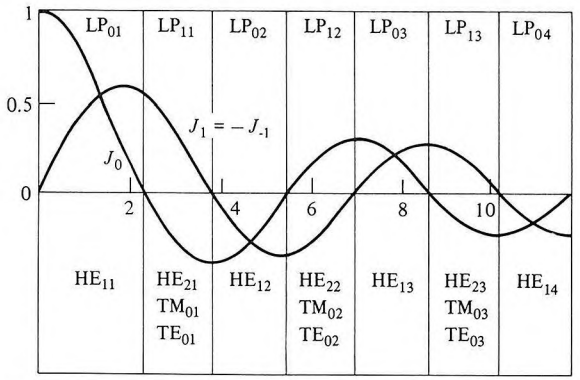

Figure 3-7 The regions of the parameter V for modes of order $l = 0, 1$.

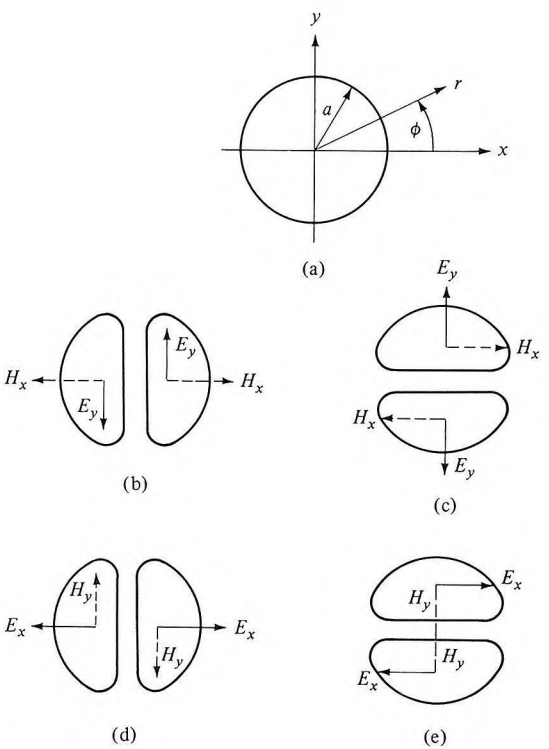

Figure 3-8 Sketch of the fiber cross section and the four possible distributions of LP_{11}.

high-order modes, the cutoff value of V is given approximately according to (3.3-28) and (3.1-13)

$$V(\mathrm{LP}_{lm}) \simeq m\pi + \left(l - \frac{3}{2}\right)\frac{\pi}{2} \tag{3.3-31}$$

Figure 3-7 shows the regions in which a given mode is the highest one allowed for a given l value group, labeled in LP mode designation. Also shown in the figure are the associated HE, EH, TE, and TM mode notations that are the exact modes. Figure 3-8 shows the field distribution of the LP_{11} modes [6]. The LP_{01} mode has radially symmetric field distribution $J_0(hr)$ in the core.

One of the most important advantages of using the linearly polarized mode is that the modes are almost transversely polarized and are dominated by one transverse electric field component (E_x or E_y) and one transverse magnetic field component (H_y or H_x). The **E** vector can be chosen to be along any arbitrary radial direction with the **H** vector along a perpendicular radial direction. Once this mode is chosen, there exists another independent mode with E and H orthogonal to the first pair.

Power Flow and Power Density

We now derive expressions for the Poynting vector and the power flow in the core and cladding. The time-averaged Poynting vector along the waveguide is, acccording to (3.1-18)

$$S_z = \tfrac{1}{2}\mathrm{Re}[E_x H_y^* - E_y H_x^*) \tag{3.3-32}$$

Substituting the field components from (3.3-18) and (3.3-19) or (3.3-24) and (3.3-25) into (3.3-32), we obtain

$$S_z = \begin{cases} \dfrac{\beta}{2\omega\mu}|A|^2 J_l^2(hr) & r < a \\ \dfrac{\beta}{2\omega\mu}|B|^2 K_l^2(hr) & r > a \end{cases} \tag{3.3-33}$$

Note that the intensity distribution is cylindrical symmetric (i.e., no ϕ-dependence). The amount of power that is contained in the core and the cladding is given by, respectively,

$$P_{\text{core}} = \int_0^{2\pi}\int_0^a S_z r\, dr\, d\phi \tag{3.3-34}$$

$$P_{\text{clad}} = \int_0^{2\pi}\int_a^{\infty} S_z r\, dr\, d\phi \tag{3.3-35}$$

Using the following integrals of Bessel functions [7]

$$\int_0^a rJ_l^2(hr)\,dr = \frac{a^2}{2}\left[J_l^2(ha) - J_{l-1}(ha)J_{l+1}(ha)\right] \tag{3.3-36a}$$

$$\int_a^\infty rK_l^2(qr)\,dr = \frac{a^2}{2}\left[-K_l^2(qa) + K_{l-1}(qa)K_{l+1}(qa)\right] \tag{3.3-36b}$$

the powers P_{core} and P_{clad} can be written, respectively,

$$P_{\text{core}} = \frac{\beta}{2\omega\mu}\pi a^2|A|^2\left[J_l^2(ha) - J_{l-1}(ha)J_{l+1}(ha)\right] \tag{3.3-37}$$

$$P_{\text{clad}} = \frac{\beta}{2\omega\mu}\pi a^2|B|^2\left[-K_l^2(qa) + K_{l-1}(qa)K_{l+1}(qa)\right] \tag{3.3-38}$$

By using (3.3-20) for B and the mode conditions (3.3-26) and (3.3-27), the power P_{clad} can be written

$$P_{\text{clad}} = \frac{\beta}{2\omega\mu}\pi a^2|A|^2\left[-J_l^2(ha) - \left(\frac{h}{q}\right)^2 J_{l-1}(ha)J_{l+1}(ha)\right] \tag{3.3-39}$$

For those ha values that are allowed by the mode condition (3.3-26) or (3.3-27), $J_{l-1}(ha)J_{l+1}(ha)$ is always negative, so that P_{clad} is always positive. The negativeness of $J_{l-1}(ha)J_{l+1}(ha)$ can be seen from (3.3-26) and (3.3-27), since the $K_l(qa)$'s are always positive. According to (3.3-37) and (3.3-39),

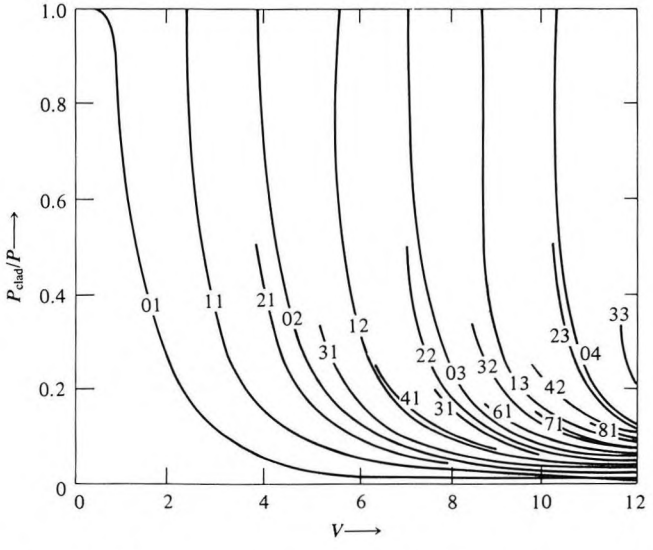

Figure 3-9 Fractional power contained in the cladding as a function of the frequency parameter V. (After Reference [5].)

the total power flow is thus given by

$$P = \frac{\beta}{2\omega\mu}\pi a^2|A|^2\left(1 + \frac{h^2}{q^2}\right)[-J_{l-1}(ha)J_{l+1}(ha)] \tag{3.3-40}$$

The ratio of cladding power to the total power, $\Gamma_2 = (P_{\text{clad}}/P)$, which measures the fraction of mode power flowing in the cladding layer, is given, according to (3.3-39) and (3.3-40), by

$$\Gamma_2 = \frac{P_{\text{clad}}}{P} = \frac{1}{V^2}\left[(ha)^2 + \frac{(qa)^2 J_l^2(ha)}{J_{l-1}(ha)J_{l+1}(ha)}\right] \tag{3.3-41}$$

where we used $(ha)^2 + (qa)^2 = k_0^2 a^2(n_1^2 - n_2^2) = V^2$. Figure 3-9 shows the ratio P_{clad}/P for several modes as a function of the normalized frequency V [5]. Note that the fundamental mode LP_{01} is best confined. Generally speaking, P_{clad}/P increases when the mode subscript lm increases.

Mode Dispersion

The propagation constant of a guided mode LP_{lm} is obtained as a solution of the mode condition (3.3-26) or (3.3-27). It is often expressed in terms of the mode index defined as

$$\beta_{lm} = n_{lm}k_0 = n_{lm}(n_1, n_2, \omega)\frac{\omega}{c} \tag{3.3-42}$$

where the mode index n_{lm} (often called effective index of mode lm) is considered as a function of n_1, n_2, and ω (see Figure 3-6). The velocity with which the mode energy in a light pulse travels down a waveguide is called the *group velocity* and is characterized by the expression

$$(v_g)_{lm} = \frac{d\omega}{d\beta_{lm}} = \left(\frac{d\beta_{lm}}{d\omega}\right)^{-1} \tag{3.3-43}$$

At a given frequency, different modes will thus have different group velocities. This is the modal dispersion discussed in Section 2.9. Pulse broadening and distortion in multimode waveguides where the energy is carried simultaneously by many modes is due mostly to modal dispersion, i.e., lm-dependence of v_g.

In single-mode waveguides (.e.g, LP_{01} mode $l = 0$, $m = 1$), modal dispersion is not operative, and the pulse broadening is caused by the group velocity dispersion alone. Dropping the subscript $lm = 01$, the group velocity in a single-mode step-index fiber can be written as

$$\frac{1}{v_g} = \frac{d\beta}{d\omega} = \frac{\omega}{c}\left(\frac{\partial n}{\partial n_1}\frac{\partial n_1}{\partial \omega} + \frac{\partial n}{\partial n_2}\frac{\partial n_2}{\partial \omega} + \frac{\partial n}{\partial \omega}\right) + \frac{n}{c} \tag{3.3-44}$$

where n_1 is the refractive index of the core, n_2 is the refractive index of the cladding, and n is the mode index. The first two terms in the square bracket

are the contribution from material dispersion, whereas the third term is a result of the waveguide dispersion. From the uniform dielectric perturbation theory, the change in the eigenvalue β^2 results from a uniform dielectric perturbation δn_1^2, and δn_2^2 in the core and cladding, respectively, is given by

$$\delta\beta^2 = \left(\frac{\omega}{c}\right)^2 (\Gamma_1 \delta n_1^2 + \Gamma_2 \delta n_2^2) \tag{3.3-45}$$

where Γ_1 and Γ_2 are the fraction of power flowing in the core and cladding, respectively. Using $\beta^2 = n^2(\omega/c)^2$, we obtain from (3.3-45)

$$\begin{aligned} \frac{\partial n}{\partial n_1} &= \Gamma_1 \left(\frac{n_1}{n}\right) \\ \frac{\partial n}{\partial n_2} &= \Gamma_2 \left(\frac{n_2}{n}\right) \end{aligned} \tag{3.3-46}$$

The group velocity can thus be expressed as

$$\frac{1}{v_g} = \frac{d\beta}{d\omega} = \frac{\omega}{c}\left[\Gamma_1 \left(\frac{n_1}{n}\right)\left(\frac{\partial n_1}{\partial \omega}\right) + \Gamma_2 \left(\frac{n_2}{n}\right)\left(\frac{\partial n_2}{\partial \omega}\right) + \left(\frac{\partial n}{\partial \omega}\right)_w\right] + \frac{n}{c} \tag{3.3-47}$$

where we put a subscript w to indicate that $(\partial n/\partial\omega)_w$ is a waveguide dispersion. In a weakly guiding fiber $n_1 \simeq n_2$, we may assume that

$$\frac{\partial n_1}{\partial \omega} \simeq \frac{\partial n_2}{\partial \omega} \equiv \left(\frac{\partial n}{\partial \omega}\right)_m \tag{3.3-48}$$

where the subscript m indicates material dispersion. The group velocity (3.3-47) can thus be written

$$\frac{1}{v_g} = \frac{d\beta}{d\omega} = \frac{\omega}{c}\left[\left(\frac{\partial n}{\partial \omega}\right)_m + \left(\frac{\partial n}{\partial \omega}\right)_w\right] + \frac{n}{c} \tag{3.3-49}$$

Using $\omega = 2\pi c/\lambda$, (3.3-49) can be written in terms of λ as

$$\frac{1}{v_g} = \frac{d\beta}{d\omega} = -\frac{\lambda}{c}\left[\left(\frac{\partial n}{\partial \lambda}\right)_m + \left(\frac{\partial n}{\partial \lambda}\right)_w\right] + \frac{n}{c} \tag{3.3-50}$$

The group velocity dispersion D is thus given, according to (2.9-33) and (3.3-49), by

$$D = -\frac{\lambda}{c}\left[\left(\frac{\partial^2 n}{\partial \lambda^2}\right)_m + \left(\frac{\partial^2 n}{\partial \lambda^2}\right)_w\right] \tag{3.3-51}$$

Note that both material dispersion and waveguide dispersion contribute to the group velocity dispersion. The second-order derivatives $(\partial^2 n/\partial\lambda^2)_{m,w}$ vanish at the point of inflection on the curve $n(\lambda)$, i.e., point where $(\partial n/\partial\lambda)_{m,w}$ is minimum or maximum. For GeO_2-doped silica, $(\partial^2 n/\partial\lambda^2)_m$ passes through zero near $\lambda = 1.3$ μm [8, 9]. The waveguide dispersion $(\partial^2 n/\partial\lambda^2)_w$ vanishes at a wavelength that depends on core diameter a as well as n_1 and n_2. It is possible to tailor the zero-dispersion wavelength in single-mode fibers by

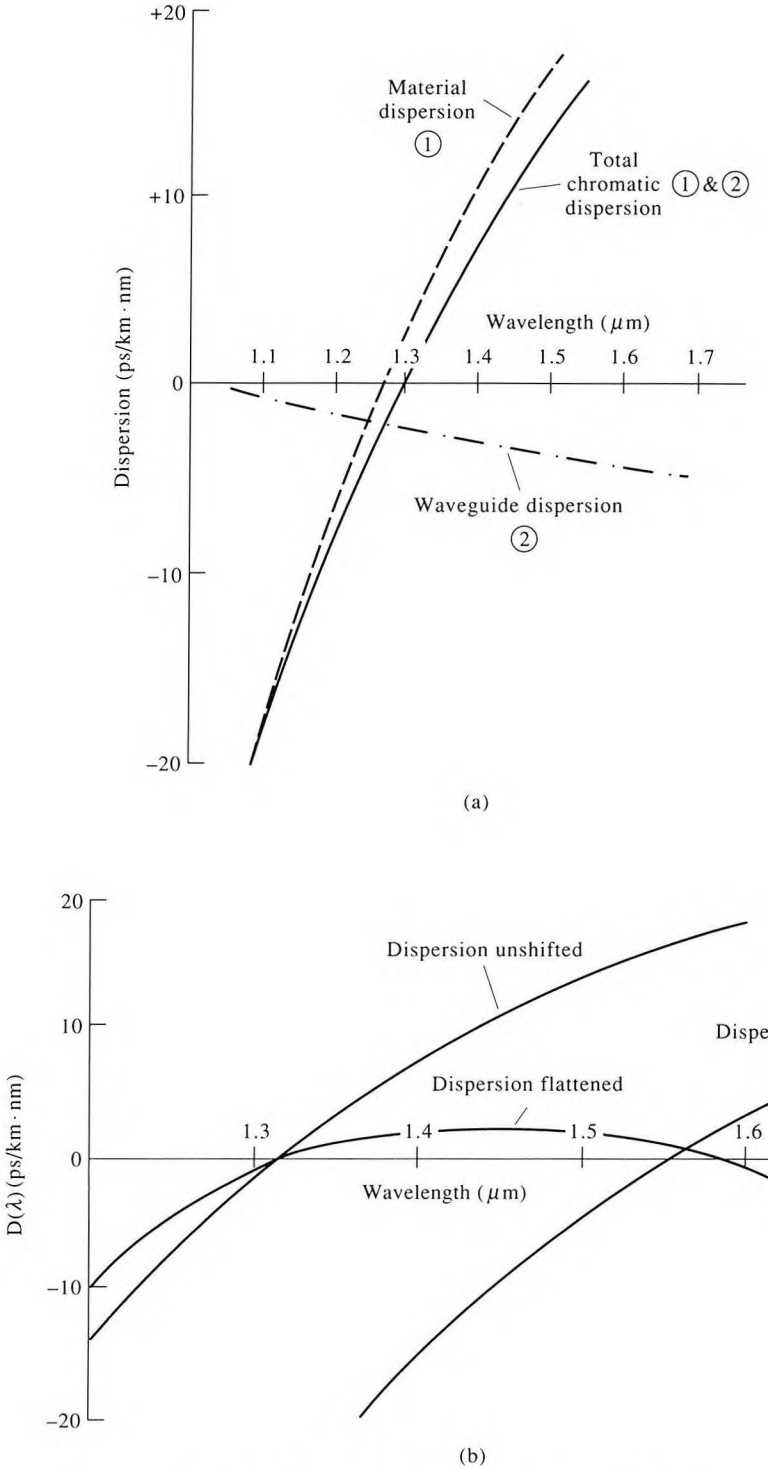

Figure 3-10 Group velocity disperion of (a) dispersion-unshifted 1.3 μm fiber and (b) dispersion-flattened and dispersion-shifted fibers. (After Reference [23].)

balancing the (negative) material dispersion against the (positive) waveguide dispersion [10]. Thus, by choosing a core diameter a between 4 and 5 μm and relative refractive index difference of $(n_1 - n_2)/n_1 > 0.004$, the wavelength of minimum group velocity dispersion can be shifted to the 1.5- to 1.6-μm region where the loss is lowest [11–16]. Figure 3-10(a) shows the waveguide and material (chromatic) contributions to the group velocity dispersion of the "conventional" 1.3 μm fibers. Figure 3-10(b) plots the dispersion curves for dispersion-shifted fibers.

3.4 GRADED-INDEX FIBERS

Referring to Figure 3-11, we now consider a circular waveguide in which the index of refraction of the core is graded. An example of such a core medium is the quadratic-index medium discussed in Chapter 2. Graded-index fibers are used in some applications because they offer a multimode propagation in a relatively large core fiber coupled with low modal dispersion. Consider the case of a power-law refractive index profile given by

$$n(r) = \begin{cases} n_1 \left[1 - 2\Delta \left(\frac{r}{a} \right)^g \right]^{1/2} & r < a \\ n_1(1 - 2\Delta)^{1/2} & r > a \end{cases} \tag{3.4-1}$$

where $\Delta = (n_1^2 - n_2^2)/2n_1^2 \simeq (n_1 - n_2)/n_1$ and g is the power-law coefficient. The case of $g = 2$ is known as the parabolic-index profile, and is the quadratic-index medium discussed in Chapter 2. In the limit when $g \to \infty$, the index profile becomes that of a step-index waveguide.

It was shown in Chapter 2 [see Table 2-1(6)] that light rays follow sinusoidally varying curved paths in the quadratic-index medium ($g = 2$). Rays that do not approach the core boundary closely can be regarded as propagating in an idealized, infinitely extended graded-index medium, as indicated by the dashed lines in Figure 3-11. For those rays, the mode analysis of such fibers is greatly simplified by assuming that the graded-index profile of the

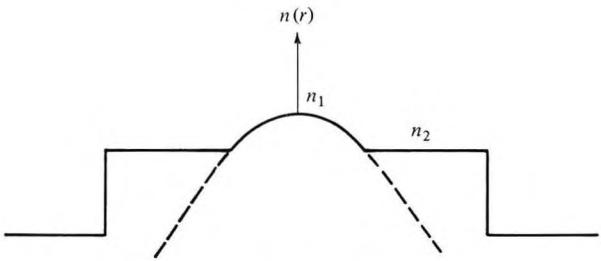

Figure 3-11 Structures and index profile of a graded-index fiber.

core continues indefinitely beyond the core region. For example, in the quadratic-index fiber [with $g = 2$ in (3.4-1)], the mode solutions are Hermite–Gaussian functions in a Cartesian coordinate (see Chapter 2) or Laguerre–Gaussian functions in cylindrical coordinates, provided the index profile continues its quadratic shape beyond $r = a$. For those well-confined modes that have most of their mode power flowing in the core region ($r < a$), it is a good approximation to assume that the index profile retains the same radial dependence beyond $r = a$. Even in this approximation, closed form solutions of the mode amplitudes can only be obtained for very few refractive index profiles. In general, only approximate solutions for the mode functions or the propagation constants can be obtained. One of the most powerful analytical methods for obtaining the approximate mode solutions and the propagation constants of graded-index fibers with arbitrary profiles is the WKB method. This method provides a good approximation for the mode amplitudes and the propagation constants whenever the index of refraction $n(r)$ does not vary appreciably over distances on the order of one wavelength. In what follows we will present some important results of the WKB approximation that are useful in deriving the propagation constants. For the detailed derivation of these results, the reader is referred to References [16–18].

The WKB Approximation

In the approximate WKB solution that follows, we take the transverse component of the linearly polarized electric field of the (LP) modes as

$$E_t = \psi(r)e^{il\phi} \exp[i(\omega t - \beta z)] \tag{3.4-2}$$

The transverse component of the magnetic field is given by

$$H_t = \frac{\beta}{\omega\mu} E_t \tag{3.4-3}$$

where the direction of the magnetic field is perpendicular to the electric field and in such a sense that gives a positive power flow in the z direction. The radial function $\psi(r)$ obeys Equation (3.1-9), which is now written as

$$\left[\frac{d^2}{dr^2} + \frac{1}{r}\frac{d}{dr} + p^2(r)\right] \psi(r) = 0 \tag{3.4-4}$$

where

$$p^2(r) = k_0^2 n^2(r) - \beta^2 - \frac{l^2}{r^2} \tag{3.4-5}$$

$p(r)$ may be interpreted as the local transverse wave number at r. The solution to the wave equation (3.4-4) is oscillatory in the region where $p^2(r) > 0$ and becomes exponential in the region where $p^2(r) < 0$. For confined modes,

$p^2(r = \infty)$ must be negative to ensure the exponential decay of the field and $p^2(r) > 0$ in some region in order to have a finite field at $r = 0$. Let r_1 and r_2 define a region $r_1 < r < r_2$ where $p^2(r) > 0$, and let $p^2(r) < 0$ elsewhere. For $l = 0$, $r_1 = 0$, and $p^2(r_2) = 0$. For $l \neq 0$, $r_1 > 0$, and $p^2(r_1) = p^2(r_2) = 0$. In the regions outside the range $r_1 < r < r_2$, the wave is evanescent. These regions are "classically inaccessible," and light is totally reflected from the surfaces $r = r_1$ and $r = r_2$.

We now take $\psi(r)$ of the form

$$\psi(r) = e^{iS(r)} \tag{3.4-6}$$

where $S(r)$ is a complex function of r. Substitution of (3.4-6) for $\psi(r)$ in (3.4-4) leads to

$$iS'' + \frac{iS'}{r} - (S')^2 + p^2(r) = 0 \tag{3.4-7}$$

where the prime indicates differentiation with respect to r. If we assume $S'' + S'/r \ll S'^2$, we obtain the first approximation for S'

$$S'(r) = \pm p(r) \tag{3.4-8}$$

This approximation is valid, provided

$$\left| p'(r) + \frac{p(r)}{r} \right| \ll |p^2(r)| \tag{3.4-9}$$

By substituting (3.4-8) for S' in the first two terms in (3.4-7), we obtain the second approximation for S'

$$(S')^2 = p^2 \pm ip' \pm \frac{ip}{r} \tag{3.4-10}$$

Using (3.4-9), S' can be written

$$S'(r) = \pm p(r) + \frac{i}{2r} + i\frac{p'}{2p} \tag{3.4-11}$$

Integration of (3.4-11) leads to

$$S(r) = \pm \int p(r)\, dr + i \ln(rp)^{1/2} \tag{3.4-12}$$

From (3.4-6) and (3.4-12), the general solution $\psi(r)$ thus takes the form

$$\psi(r) = \frac{1}{[rp(r)^{1/2}} \left\{ c_1 \exp\left[i \int p(r)\, dr \right] + c_2 \left[-i \int p(r)\, dr \right] \right\} \tag{3.4-13}$$

where c_1 and c_2 are arbitrary constants. This solution (3.4-13) is not valid at the turning points where $p(r) = 0$ because at these points the assumption

(3.4-9) fails. The true form of the solution near the turning points must be obtained independently by expanding $p^2(r)$ near these points as Taylor series and then solving the Equation (3.4-4). By matching these solutions with (3.4-13), the constants can be determined. The results are [17–19]

$$\psi(r) = \begin{cases} \dfrac{A}{[rp(r)]^{1/2}} \exp\left[-\displaystyle\int_r^{r_1} |p(r)|\, dr\right] & r < r_1 \qquad \text{(3.4-14a)} \\ \dfrac{B}{[rp(r)]^{1/2}} \sin\left[\displaystyle\int_{r_1}^{r} p(r)\, dr + \frac{\pi}{4}\right] & r_1 < r \qquad \text{(3.4-14b)} \end{cases}$$

$$\psi(r) = \begin{cases} \dfrac{C}{[rp(r)]^{1/2}} \sin\left[\displaystyle\int_r^{r_2} p(r)\, dr + \frac{\pi}{4}\right] & r < r_2 \qquad \text{(3.4-15a)} \\ \dfrac{D}{[rp(r)]^{1/2}} \exp\left[-\displaystyle\int_{r_2}^{r} |p(r)|\, dr\right] & r_2 < r \qquad \text{(3.4-15b)} \end{cases}$$

Since (3.4-14b) and (3.4-15a) represent the field solution in the same region, the uniqueness of the field requires that

$$B \sin\left[\int_{r_1}^{r} p(r)\, dr + \frac{\pi}{4}\right] = C \sin\left[\int_r^{r_2} p(r)\, dr + \frac{\pi}{4}\right] \qquad \text{(3.4-16)}$$

Using $\sin[(m+1)\pi - \alpha] = (-1)^m \sin\alpha$, the equality (3.4-16) requires that the sum of their phases be an integral multiple of π, i.e.,

$$\int_{r_1}^{r_2} p(r)\, dr + \frac{\pi}{2} = (m+1)\pi \qquad \text{(3.4-17)}$$

and $C = (-1)^m B$. Equation (3.4-17) is often written as

$$\int_{r_1}^{r_2} p(r)\, dr = (m + \tfrac{1}{2})\pi \qquad m = 0, 1, 2, \ldots \qquad \text{(3.4-18)}$$

and is known as the Bohr–Sommerfeld quantization rule of the old quantum theory [19]. By using (3.4-5), the mode condition (3.4-18) becomes

$$\int_{r_1}^{r_2} \left[k_0^2 n^2(r) - \beta^2 - \frac{l^2}{r^2}\right]^{1/2} dr = (m + \tfrac{1}{2})\pi \qquad \text{(3.4-19)}$$

The mode condition (3.4-19) again can be solved for β in closed analytical form only for a few simple refractive index profiles. In most general cases it must be solved numerically or approximately.

Example: WKB Solutions for the Propagation Constants of Quadratic-Index Fiber

We consider a fiber with parabolic-index profile

$$n(r) = n_1 \left[1 - 2\Delta \left(\frac{r}{a} \right)^2 \right]^{1/2} \tag{3.4-20}$$

Substituting $n(r)$ into the mode condition (3.4-19), we obtain

$$\frac{n_1 k_0 \sqrt{2\Delta}}{a} \int_{r_1}^{r_2} \frac{\sqrt{(r_2^2 - r^2)(r^2 - r_1^2)}}{r} \, dr = (m + \tfrac{1}{2})\pi \tag{3.4-21}$$

where r_1 and r_2 are roots of $p^2(r) = 0$ (i.e., the turning points). Using the substitution $u = r^2$ and the integral formula

$$\int_a^b \frac{\sqrt{(b - x)(x - a)}}{x} \, dx = \left(\frac{a + b}{2} - \sqrt{ab} \right) \pi \qquad ab > 0 \tag{3.4-22}$$

The mode condition (3.4-21) becomes

$$\left(\frac{k_0^2 n_1^2 - \beta^2}{(2n_1 k_0 \sqrt{2\Delta})/a} - |l| \right) \frac{\pi}{2} = (m + \tfrac{1}{2})\pi \qquad m = 0, 1, 2, \ldots \tag{3.4-23}$$

Solving (3.4-23) for β, we obtain

$$\beta = n_1 k_0 \left[1 - \frac{2(2\Delta)^{1/2}}{n_1 k_0 a} (|l| + 2m + 1) \right]^{1/2} \tag{3.4-24}$$

The WKB value (3.4-24) of the propagation constant β of the quadratic-index fiber modes is identical to that given by the exact solution of the wave equation (2.9-13). In using (3.4-24) we must keep in mind that (3.4-24) is obtained by assuming an index profile of the form (3.4-20) for all r. In practice the parabolic-index profile is truncated at the core boundary $r = a$. Therefore, a confined mode must have its propagation constant larger than $n_1(1 - 2\Delta)^{1/2} k_0$ (i.e., $n_1(1 - 2\Delta)^{1/2} k_0 < \beta < n_1 k_0$). Thus the mode subscripts (quantum numbers) l and m are limited by the following condition:

$$2(|l| + 2m + 1) \leq n_1 k_0 a \sqrt{2\Delta} = k_0 a (n_1^2 - n_2^2)^{1/2} \tag{3.4-25}$$

where n_2 is the clad refractive index $n_2 = n_1(1 - 2\Delta)^{1/2}$. Note that this n_2 is not to be confused with n_2 defined in Chapter 2 [Equation (2.9-1a)].

3.5 ATTENUATION IN SILICA FIBERS

Probably the single most important factor responsible for the emergence of the silica glass optical fiber as a premium transmission medium is the low optical propagation losses in such fibers. Figure 3-12 shows the measured

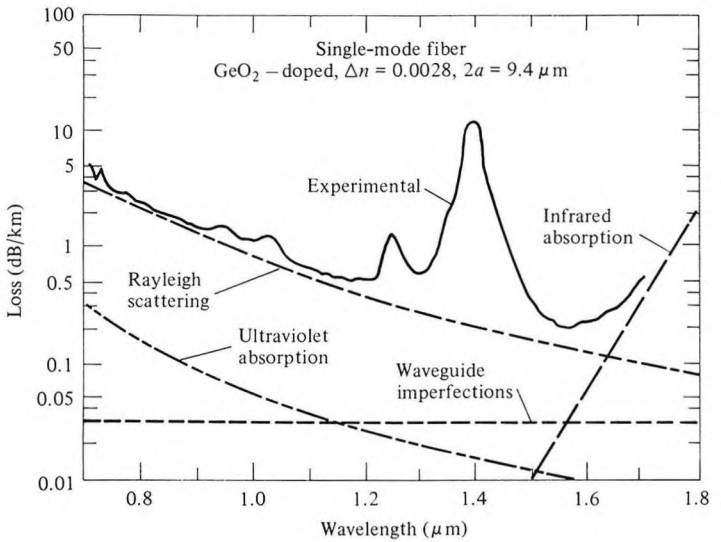

Figure 3-12 Observed loss spectrum of a germanosilicate single-mode fiber. Estimated loss spectra for various intrinsic materials effects and waveguide imperfections are also shown. (From Reference [20].)

losses as a function of wavelength of a high-quality, germania-doped single-mode fiber. The loss peak around 1.4 μm is due to residual OH contamination of the glass. A low value of loss ~0.2 dB/km obtains near $\lambda = 1.55\ \mu$m. Consequently, this region of the spectrum is now favored for long-distance optical communication. Recent experiments have taken advantage of the small pulse spreading near the zero group velocity dispersion wavelength and the low losses to demonstrate high-data-rate transmission (data rate exceeding 400 Mb/s) over a propagation path exceeding 100 km [20, 21] at $\lambda \sim 1.55\ \mu$m.

For a more detailed discussion of propagation effects in optical fibers, the student can consult Reference [22].

Problems

3.1 The number of confined modes that can be supported by a circular dielectric waveguide depends on the refractive-index profile and the wavelength.

a. Using the cutoff value for the LP_{lm} mode, show that the mode subscripts (l, m) for a step-index fiber must satisfy the condition

$$m\pi + \left(l - \frac{3}{2}\right)\frac{\pi}{2} \leq V$$

where $V = k_0 a(n_1^2 - n_2^2)^{1/2}$. Show that each LP_{lm} mode is fourfold degenerate.

b. By counting the allowed mode subscripts (l, m), show that the total number of confined modes that can be supported by a step-index fiber is

$$N \simeq \frac{4}{\pi^2} V^2 \simeq \frac{1}{2} V^2$$

c. Using (3.4-25) show that for a truncated quadratic-index fiber

$$N \simeq \tfrac{1}{4} V^2$$

Note that the total number of modes in a truncated quadratic-index fiber is one-half of that of a step-index fiber.

d. Estimate the number of confined modes in a multimode step-index fiber with $a = 50\ \mu\mathrm{m}$, $n_1 = 1.52$, $n_2 = 1.50$ at a carrier wavelength of $\lambda = 1\ \mu\mathrm{m}$.

e. In a general, truncated graded-index fiber with a core radius a and a cladding index n_2, it is convenient to define an effective V number such that

$$V_{\mathrm{eff}}^2 = 2k_0^2 \int_0^a [n^2(r) - n_2^2] r\, dr$$

and the number of confined modes is approximately given by

$$N \simeq \tfrac{1}{2} V_{\mathrm{eff}}^2$$

Show that this approximation agrees with (b) and (c) for step-index and quadratic-index fibers, respectively.

f. Show that, according to (e), the number of confined modes in a power-law graded-index fiber with an index profile given by (3.4-1) is

$$N = \frac{1}{2(1 + 2/g)} V^2 = \frac{k_0^2 a^2}{2(1 + 2/g)} (n_1^2 - n_2^2)$$

Show that this expression again agrees with the results obtained in (b) for step-index fibers ($g = \infty$) and in (c) for quadratic-index fibers ($g = 2$).

3.2 The numerical aperture (NA) is a measure of the light-gathering capability of a fiber. It is defined as the sine of the maximum external angle of the entrance ray (measured with respect to the axis of fiber) that is trapped in the core by total internal reflection.

a. Show that

$$\mathrm{NA} = n_1 \sin \theta_1 = (n_1^2 - n_2^2)^{1/2}$$

b. Show that the solid acceptance angle in air is

$$\Omega = \pi(n_1^2 - n_2^2) = \pi(\mathrm{NA})^2$$

c. Show that the solid angle (in air) for a single electromagnetic radiation mode leaving or entering the core aperture is

$$\Omega_{\text{mode}} = \frac{\lambda^2}{\pi a^2}$$

d. The total number of modes the fiber can support, couple to, and radiate into air is therefore

$$N = 2\,\frac{\Omega}{\Omega_{\text{mode}}}$$

where 2 accounts for the two independent polarizations in air. Show that this estimate agrees with Problem 3.1.

e. Find the numerical aperture of a multimode fiber with $n_1 = 1.52$ and $N_2 = 1.50$.

3.3 A single-mode step-index fiber must have a V number less than 2.405; i.e.,

$$V = k_0 a(n_1^2 - n_2^2)^{1/2} < 2.405$$

a. Show that the expression derived in Problem 3.1(b) ($N \simeq 4V^2/\pi^2$) still applies, provided we realize that a single-mode fiber supports two independently polarized HE_{11} modes (or LP_{01} modes).
b. With $a = 5\ \mu$m, $n_2 = 1.50$, and $\lambda = 1\ \mu$m, find the maximum core index for a single-mode fiber. (*Answer*: $n_1 = 1.50195$.)
c. With $n_1 = 1.501$, $n_2 = 1.500$, and $\lambda = 1\ \mu$m, find the maximum core radius for a single-mode fiber. (*Answer*: $a = 7\ \mu$m.)
d. Show that the confinement factor for a single-mode fiber is

$$\Gamma_1 = \frac{P_{\text{core}}}{P} = \frac{(qa)^2}{V^2}\left(1 + \frac{J_0^2(ha)}{J_1(ha)}\right)$$

where ha satisfies the mode condition (3.3-26)

$$ha\,\frac{J_1(ha)}{J_0(ha)} = qa\,\frac{K_1(qa)}{K_0(qa)}$$

e. Show that, by using the table of Bessel functions, $ha = 1.647$ is an approximate solution to the mode condition for $V = 2.405$. Evaluate the confinement factor Γ_1 for the LP_{01} mode of this single-mode fiber (*Answer*: $\Gamma_1 = 83\%$). Note that this is the maximum confinement factor for a single-mode fiber. Compare this value with the curves in Figure 3-9.

3.4 Mode condition

a. Derive the mode condition for step-index fibers (3.2-11).
b. Derive the expressions for the constants B, C, D, in terms of A (3.2-12).

c. Derive the mode conditions for TE and TM modes (3.2-17).
d. Show that $E_z = E_r = 0$ for TE modes and $H_z = H_r = 0$ for TM modes.
e. Show that in the limit $n_1 - n_2 \ll n_1$, TE and TM modes become identical.

3.5

a. Derive (3.3-6) and (3.3-7).
b. Derive (3.3-18) and (3.3-19).
c. Derive (3.3-23).
d. Derive (3.3-24) and (3.3-25).

References

1. Kao, C. K., and T. W. Davies, "Spectroscopic studies of ultra low loss optical glasses," *J. Sci. Instrum.* 1(no. 2):1063, 1968.
2. Kapron, F. P., D. B. Keck, and R. D. Maurer, "Radiation losses in glass optical waveguides," *Appl. Phys. Lett.* 17:423, 1970.
3. Snitzer, E., "Cylindrical dielectric waveguide modes," *J. Opt. Soc. Am.* 51:491, 1961.
4. Keck, D. B., *Fundamentals in Optical Fiber Communications* (M. K. Barnoski, ed.). New York: Academic Press, 1976, Chapter 1.
5. Gloge, D., "Weakly guiding fibers," *Appl. Opt.* 10:2252, 1971.
6. See, for example, D. Marcuse, *Theory of Dielectric Optical Waveguides*. New York: Academic Press, 1974.
7. See, for example, I. S. Gradshteyn and I. M. Ryzhik, *Table of Integrals, Series, and Products*. New York: Academic Press, 1965, p. 634, Eq. (5.54-2).
8. Payne, D. N., and W. A. Gambling, "Zero material dispersion in optical fibers," *Electron. Lett.* 11:176, 1975.
9. Cohen, L. G., and C. Lin, "Pulse delay measurements in the zero material dispersion wavelength region for optical fibers," *Appl. Opt.* 12:3136, 1977.
10. Li, T., "Structures, parameters, and transmission properties of optical fibers," *Proc. IEEE* 68:1175, 1980.
11. Cohen, L. G., W. L. Mammel, and H. M. Presby, "Correlation between numerical predications and measurements of single-mode fiber dispersion characteristics," *Appl. Opt.* 19:2007, 1980.
12. Tsuchiya, H., and N. Imoto, "Dispersion-free single mode fibers in 1.5 μm wavelength region," *Electron. Lett.* 15:476, 1979.
13. Cohen, L. G., C. Lin, and W. G. French, "Tailoring zero chromatic dispersion into the 1.5–1.6 μm low-loss spectral region of single-mode fibers," *Electron. Lett.* 15:334, 1979.
14. White, K. I., and B. P. Nelson, "Zero total dispersion in step-index monomode fibres at 1.30 and 1.55 m," *Electron. Lett.* 15:396, 1979.
15. Gambling, W. A., H. Matsumara, and C. M. Ragdale, "Zero total dispersion in graded-index single-mode fibers," *Electron. Lett.* 15:474, 1979.

16. Yamada, J. I., et al., "High speed optical pulse transmission at 1.29 μm wavelength using low loss single mode fibers," *IEEE J. Quantum Electron. QE-14*:791, 1978.
17. Morse, P. M., and H. Feshbach, *Methods of Theoretical Physics*. New York: McGraw-Hill, 1953.
18. Mathews, J., and R. L. Walker, *Mathematical Methods of Physics*. New York: Benjamin, 1965.
19. Landau, L. D., and E. M. Lifshitz, *Quantum Mechanics*. London: Pergamon Press, 1958.
20. Miya, T., Y. Terunuma, T. Hosaka, and T. Miyashita, "Ultimate low-loss single-mode fiber at 1.55 μm," *Electron. Lett.* 15:106, 1979.
21. Suematsu, Y., "Long wavelength optical fiber communication," *Proc. IEEE* 71:692, 1983.
22. Miller, S., and I. P. Kaminow, ed., *Optical Fiber Telecommunication II*. San Diego: Academic Press, 1988, Chapters 2 and 3.
23. Figure 3-10(a) is courtesy of S. R. Nagel, AT&T Bell Laboratories. Figure 3-10(b) is from D. L. Frazen, "Single mode fiber measurements," *Proceedings of the Tutorial Sessions Conference on Optical Fiber Communications*. Washington, D.C., Opt. Soc. Am., 1988, p. 101.